

Finite element analysis of mechanical properties of 2.5D angle-interlock woven composites: Part 1— Full-cell model and its validation

Jian Song^a, Weidong Wen & Haitao Cui

Jiangsu Province Key Laboratory of Aerospace Power System, College of Energy and Power Engineering,
Nanjing University of Aeronautics and Astronautics, Nanjing, Jiangsu 210016, China

Received 5 October 2014; revised received and accepted 24 February 2015

A new parameterized micro-structural model of 2.5D angle-interlock woven composites, named 'full-cell model', has been established. In order to verify the validation of finite element model (FEM) based on the full-cell model, the effective elastic properties and the mechanical response of 2.5D woven composites are presented. Additionally, the effects of fibre aggregation density and thickness on the mechanical properties are also investigated in detail. The experimental results are compared with the values of FEM based on the full-cell model and inner-cell model.

Keywords: 2.5D woven composites, Carbon fibre, Finite element analysis, Full-cell model, Inner-cell model, Mechanical properties

1 Introduction

Textile composite material has been applied in advanced engineering, owing to their good comprehensive mechanics performance. In such textile composites, 2.5D angle-interlock woven composite material, possessing more simple woven technology in comparison with other 3D composites, has been applied in aeronautics and aerospace fields. Thus, it is of great importance to study the microstructure and prediction method of this kind of 2.5D woven composites¹.

Until now, the selective averaging method based on iso-stress assumption proposed by Sankar and Marrey² was used to predict the thermo-elastic properties of textile composites. Later, Zheng³ and Qiu⁴ predicted the elastic modulus of 2.5D woven composites based on this numerical method. Hallal and Younes⁵ proposed an analytical model, called three stages homogenization method, to predict the elastic properties of 2.5D composites. Jiang *et al.*⁶ studied the effective modulus of 2D textile composites using a stress and strain averaging approach. Tan *et al.*⁷ proposed a new numerical method, named as XYZ-model, according to a mixed iso-stress and iso-strain to predict the thermo-elastic properties of 3D woven composites. Ishikawa and Chou⁸⁻¹⁰ proposed the bridging model, which was

used to analyze the elastic behaviors of 2D woven composites. Meanwhile, finite element method (FEM) has also been used to estimate the mechanical properties of textile composites. Lu *et al.*^{11,12} studied the failure behaviors of 2.5D textile composites based on FEM. Li and Dong¹³ studied the stiffness, strength and damage progressive analysis of 2.5D woven composites, which neglected the influence of the outmost layer structure. Although several works have been carried out to analyze the mechanical properties of 2.5D textile composites by FEM, most of the models only considered internal structure, which inevitably introduces error. Meanwhile, the reasonable periodic boundary conditions also need to be studied.

The aim of this work is to develop accurate 3D finite element model, considering the outmost layer structure for 2.5D woven composites. And then the periodic boundary conditions for the Full-cell model are elaborately given. Finally, the influences of fibre aggregation density and thickness on the elastic properties of this material are investigated in detail and the validation of FEM will be further verified by comparing the test results.

2 Materials and Methods

The material under investigation is a 2.5D woven carbon fibre-reinforced thermosetting resin composites. The woven fabric is manufactured using fibre yarns that consist of T300-3K carbon fibres and

^aCorresponding author.
E-mail: dfsongjian2006@126.com

the matrix is QY8911-IV with a glass transition temperature 256°C. The specimens with six plies of wefts were fabricated by a resin transfer molding (RTM) technique and the corresponding diaphragm-curing process of RTM technique is shown in Fig. 1(a). The composite panel with a fibre volume fraction of 40.53% was finally obtained, and the average thickness of the panel is found about 1.88mm.

The specimens with nominal dimensions of 300 mm×25mm were cut from the woven composite panel using an abrasive water-jet cutting technique. The aluminum end tabs (50mm length) were bonded to each specimen as illustrated in Fig. 1(b). For the specimens shown in Fig. 1(b), the warp interlocks with two layers of weft in the thickness direction and the linear density is 198g /1000m. The warp (weft) arranged density in the fabric is 10 (3.5) tow/cm. The

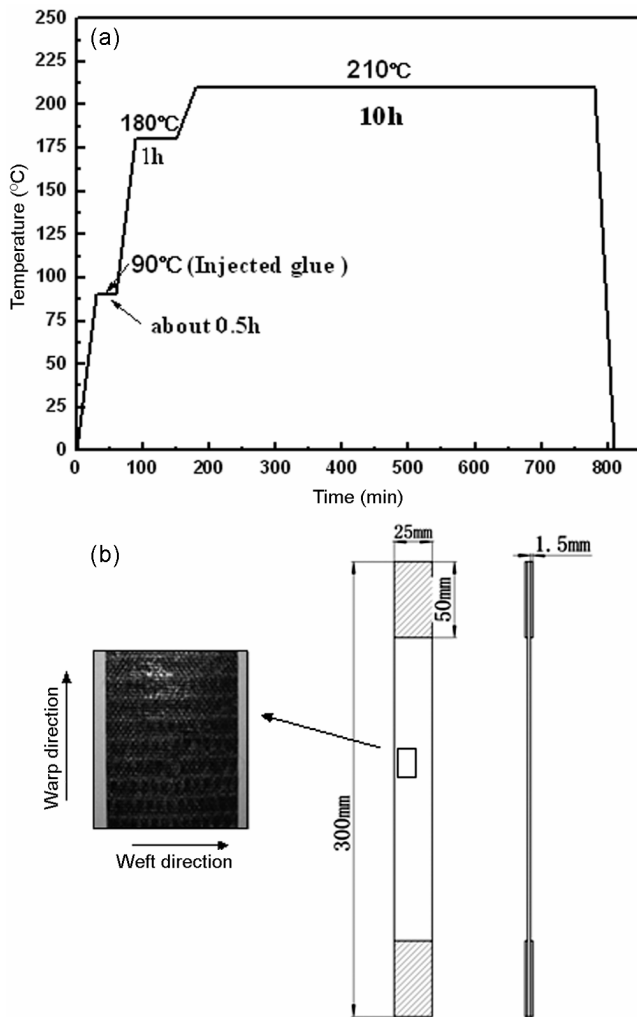


Fig. 1—Photographs of material and process (a) diaphragm-curing process of specimens, and (b) 2.5D woven composites

micro-structure observed by HIROX (Japan) microscope is shown in Fig. 2.

Due to the woven technique, a periodic structure can be obtained by ensuring that the arranged density in warp and weft directions is constant. According to Fig. 2, the minimal periodic microstructure concludes five tow wefts at the same height along the thickness direction. Furthermore, owing to the influence of molding pressure, the outmost layer weft (defined as the end weft) deviates the center line of the internal weft (named as the Inner weft), which leads to the fact that the outmost layer wefts are different with the internal layer wefts. Thus, the outmost wefts related to four layers are called the outer weft and the internal wefts are known as the middle inner weft. The configuration of end wefts are determined by three aspects, viz the outermost layer warp (closed to horizontal) and the two secondary layer warps which are upward or downward extension. Similarly, the middle inner or outer wefts are generated by four warps, viz two upward warps and two downward warps.

2.1 Finite Element Model

In order to establish the finite element model of 2.5D woven composites based on the actual microstructure as shown in Fig. 2, following three assumptions were made:

- (i) A rectangular and two anti-quadratic curve shapes are selected to describe the cross-sections of warps and wefts respectively.
- (ii) The wefts are assumed to be straight, but the trend of warp is composed of two parts [Fig. 3(b)], viz a quadratic curve depending on the

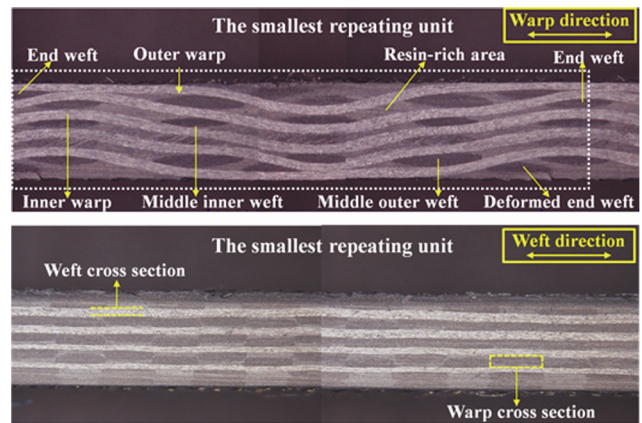


Fig. 2—Cross-sectional photomicrographs of 2.5D angle-interlock woven composites (a) longitudinal cross-section, and (b) transverse cross-section

configuration of weft and a straight line reflecting the tightening effect in the woven process.

- (iii) The yarn is treated as a unidirectional composite composed of fibre and matrix where the interface between fibre and matrix is ideal.

The model parameters shown in Fig. 3 can be calculated as follows (axes x , y , z are defined as longitudinal, transverse and thickness direction):

- The boundary dimensions of the inner cell

$$L_x = 10(N_f - 1) / M_w, \quad L_y = 10N_j / M_j \quad \dots (1)$$

where L_x and L_y are the longitudinal and transverse length (mm) respectively; N_f , the number of weft yarn at the same height in which $N_f=5$ (N_j means the number of warp yarn in the transverse direction, in which $N_j=2$); and M_j and M_w , the warp and weft arranged densities respectively.

- The cross-sectional sizes of the warp

$$A_j = \frac{T}{1000\rho P_j}, \quad W_{1j} = \frac{10}{M_j}, \quad W_{2j} = \frac{A_j}{W_{1j}} \quad \dots (2)$$

where A_j is the cross-sectional area of warp (mm^2); T , the linear density of yarns ($\text{g}/1000\text{m}$); ρ , the material density (g/cm^3); and P_j , the fibre aggregation density.

- The cross-sectional sizes of the weft and inclination angle

$$A_w = \frac{T}{1000\rho P_w}, \quad W_{2w} = \frac{L_z - (N_h + 1)W_{2j}}{N_h - 2} \quad \dots (3)$$

where A_w is the cross-sectional area of weft (mm^2); and L_z , the height in the thickness direction.

In order to obtain the width of weft yarn W_{2w} , and the inclination angle of the straight segment of the warp, a series of equations [Eqs (4)- (8)] are desired, as shown hereunder.

Firstly, based on the aforementioned assumption, the configuration of weft is assumed quadratic curve as shown below:

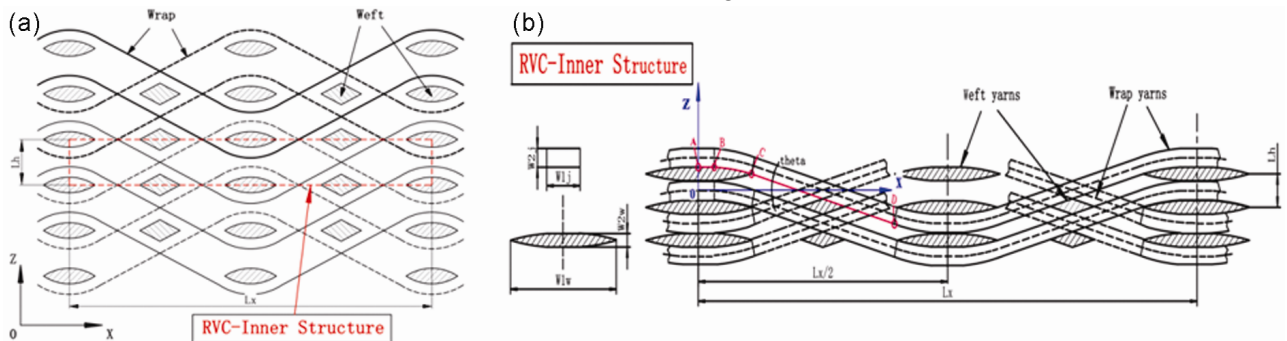


Fig. 3—Schematic diagram of internal structure (the inner-cell model) (a) microstructure of 2.5D woven composites without the outer layer structure, and (b) geometric relation in the inner structure (local amplification)

$$z = ax^2 + bx + c \quad \dots (4)$$

Next, a condition of the first-order continuous in point C (Fig. 3) must be satisfied to ensure the smooth transition in that point:

$$z'|_{x=W_{1w}/2} = -\tan\theta = 2a \cdot \frac{W_{1w}}{2} \quad \dots (5)$$

where θ is the inclination angle. Meanwhile, the inclination angle can also be described by using following relationship:

$$\tan\theta = \frac{W_{2j} + W_{2w} + W_{2j} \cos\theta}{L_x / 2 - W_{1w} - W_{2j} \sin\theta} \quad \dots (6)$$

By Eq.(6), the inclination angle can be calculated by the bisection method. Furthermore, according to the continuity condition in point C, following equation can be obtained:

$$\frac{W_{2j} + W_{2w}}{2} = a\left(\frac{W_{1w}}{2}\right)^2 + b\left(\frac{W_{1w}}{2}\right) + c \quad \dots (7)$$

Finally, the configuration of weft is obtained by adjusting W_{1w} to make sure that the area of weft is equal to A_w :

$$4 \int_0^{W_{1w}/2} \left(ax^2 + bx + c - \frac{W_{2j} + W_{2w}}{2} \right) dx = A_w \quad \dots (8)$$

Therefore, the shape parameters (W_{1w} , a , c and θ) can be calculated according to simultaneous Eqs (4)-(8). Ultimately, the inner-cell model can be established by the above parameters (Fig. 4).

The full-cell model can be established based on the inner-cell model. Figure 5(a) illustrates the forming process of 2.5D woven composites based on RTM technology. Based on the assumptions, the processing characteristic as mentioned above and the inner-cell model, a new model with outmost layer structure can be established in this work as illustrated in Fig. 5(b).

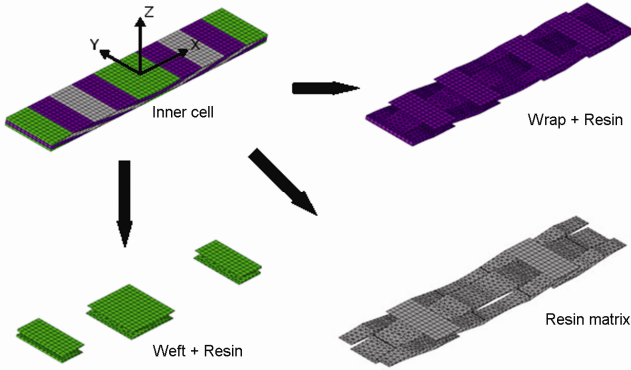


Fig. 4—Inner-cell model of 2.5D angle-interlock woven composites

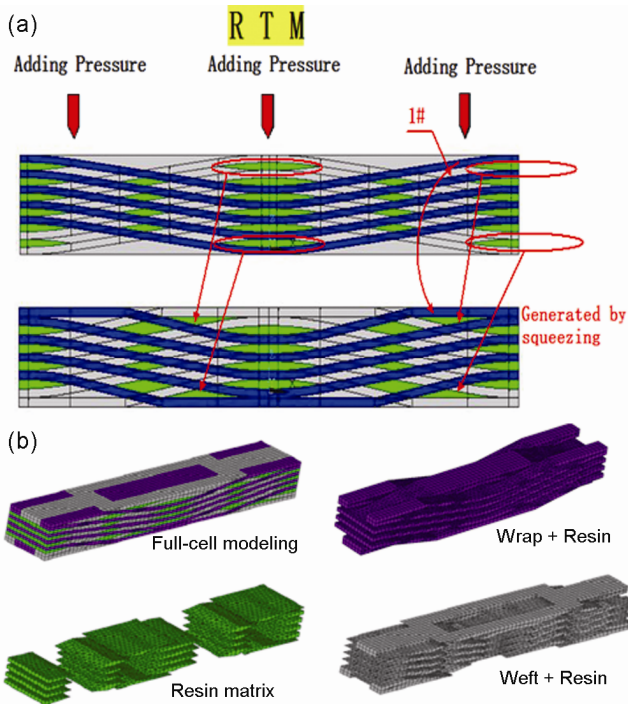


Fig. 5—(a) Molding process of 2.5D woven composites based on RTM technology and (b) full-cell model of 2.5D angle-interlock woven composites

2.2 Boundary Conditions of FEM

2.5D angle-interlock woven composites can be envisaged as a periodical array of structure. Thus, the reasonable periodic boundary conditions for the representative volume cell (RVC), which consider six independent macroscopic deformational cases ($\epsilon_x, \epsilon_y, \epsilon_z, \gamma_{xy}, \gamma_{xz}, \gamma_{yz}$) are studied as follows.

Xia¹⁴ proposed explicit forms of periodic boundary conditions based on the above general expression. This is for any parallelepiped RVC models, such as a

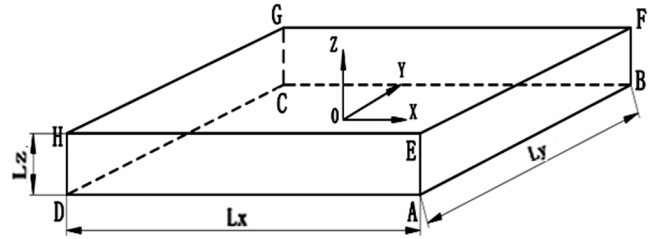


Fig. 6—Cuboid-shaped unit and its geometric dimensions

cubic structure. The following unified periodic boundary conditions are obtained:

$$u_i^{j+}(x, y, z) - u_i^{j-}(x, y, z) = c_i^j \quad (i, j = 1, 2, 3) \quad \dots (9)$$

where c_1^1, c_2^2 and c_3^3 correspond to the normal deformations, whereas the other three pairs of constants, $c_1^2(c_2^1), c_1^3(c_3^1)$ and $c_2^3(c_3^2)$ correspond to the shear deformations.

To describe Eq.(9) in the FEM software, the periodic boundary conditions are achieved by using the discrete nodes which exist in the opposite surfaces, edges and vertices of the cubic RVC model. All of the constraint equations applied in the FEM software will be given in accordance with the cubic structure (Fig. 6), as shown below:

- For three groups of the opposite surfaces:

- (i) opposite surfaces perpendicular to X axis

$$\begin{cases} u|_{x=L_x/2} - u|_{x=-L_x/2} = L_x \epsilon_x \\ v|_{x=L_x/2} - v|_{x=-L_x/2} = 0 \\ w|_{x=L_x/2} - w|_{x=-L_x/2} = 0 \end{cases} \quad \dots(10)$$

- (ii) opposite surfaces perpendicular to Y axis

$$\begin{cases} u|_{y=L_y/2} - u|_{y=-L_y/2} = L_y \gamma_{xy} \\ v|_{y=L_y/2} - v|_{y=-L_y/2} = W_y \epsilon_y \\ w|_{y=L_y/2} - w|_{y=-L_y/2} = 0 \end{cases} \quad \dots(11)$$

- (iii) opposite surfaces perpendicular to Z axis

$$\begin{cases} u|_{z=L_z/2} - u|_{z=-L_z/2} = L_z \gamma_{xz} \\ v|_{z=L_z/2} - v|_{z=-L_z/2} = L_z \gamma_{yz} \\ w|_{z=L_z/2} - w|_{z=-L_z/2} = L_z \epsilon_z \end{cases} \quad \dots(12)$$

- For twelve edges divided into three types, namely (i) AD, BC, FG and EH parallel to X axis. (ii) CD, BA, EF and HG parallel to Y axis, and (iii)HD, EA, FB and GC parallel to Z axis. The edges parallel to X axis are

$$\left\{ \begin{array}{l} u|_{BC} - u|_{AD} = L_y \gamma_{xy} \\ v|_{BC} - v|_{AD} = L_y \varepsilon_y \\ w|_{BC} - w|_{AD} = 0 \end{array} \right\}, \left\{ \begin{array}{l} u|_{FG} - u|_{AD} = L_y \gamma_{xy} + L_z \gamma_{xz} \\ v|_{FG} - v|_{AD} = L_y \varepsilon_y + L_z \gamma_{yz} \\ w|_{FG} - w|_{AD} = L_z \varepsilon_z \end{array} \right\} \dots (13)$$

$$\left\{ \begin{array}{l} u|_{EH} - u|_{AD} = L_z \gamma_{xz} \\ v|_{EH} - v|_{AD} = L_z \gamma_{yz} \\ w|_{EH} - w|_{AD} = L_z \varepsilon_z \end{array} \right. \dots (13)$$

For the other edges, the corresponding periodic boundary conditions can be obtained [Eq.(13)].

- For eight vertices, the constraint equations are established between the vertex D and the rest of vertices. The vertices of E, F, G and D are

$$\left\{ \begin{array}{l} u|_E - u|_D = L_x \varepsilon_x + L_z \gamma_{xz} \\ v|_E - v|_D = L_z \gamma_{yz} \\ w|_E - w|_D = L_z \varepsilon_z \end{array} \right\}, \left\{ \begin{array}{l} u|_F - u|_D = L_x \varepsilon_x + L_y \gamma_{xy} + L_z \gamma_{xz} \\ v|_F - v|_D = L_y \varepsilon_y + L_z \gamma_{yz} \\ w|_F - w|_D = L_z \varepsilon_z \end{array} \right\}$$

$$\left\{ \begin{array}{l} u|_G - u|_D = L_y \gamma_{xy} + L_z \gamma_{xz} \\ v|_G - v|_D = L_y \varepsilon_y + L_z \gamma_{yz} \\ w|_G - w|_D = L_z \varepsilon_z \end{array} \right. \dots (14)$$

For the other vertices, the corresponding periodic boundary conditions can be obtained using Eq. (14).

According to the discrete method, it is convenient to achieve the boundary conditions in FEM software. In addition, assume that the average mechanical properties of a RVC are equal to the average properties of 2.5D woven composites. The average stresses are defined as:

$$\bar{\sigma}_{ij} = \frac{1}{V} \int_V \sigma_{ij} dV = \frac{P_{ij}}{S_j}, (\text{no summation over } j) \dots (15)$$

For the full-cell model, since the upper and lower boundary is the actual boundary of the 2.5D woven composites, the periodic boundary condition mentioned above can be simplified; the boundary condition neglecting the equations corresponding to the Z direction.

3 Results and Discussion

3.1 Stress Nephogram Based on the Full-cell Model

Figure 7 illustrates the stress nephograms based on the full-cell model and Inner-cell model subjected to the warp, weft and in-plane shear tensile loadings.

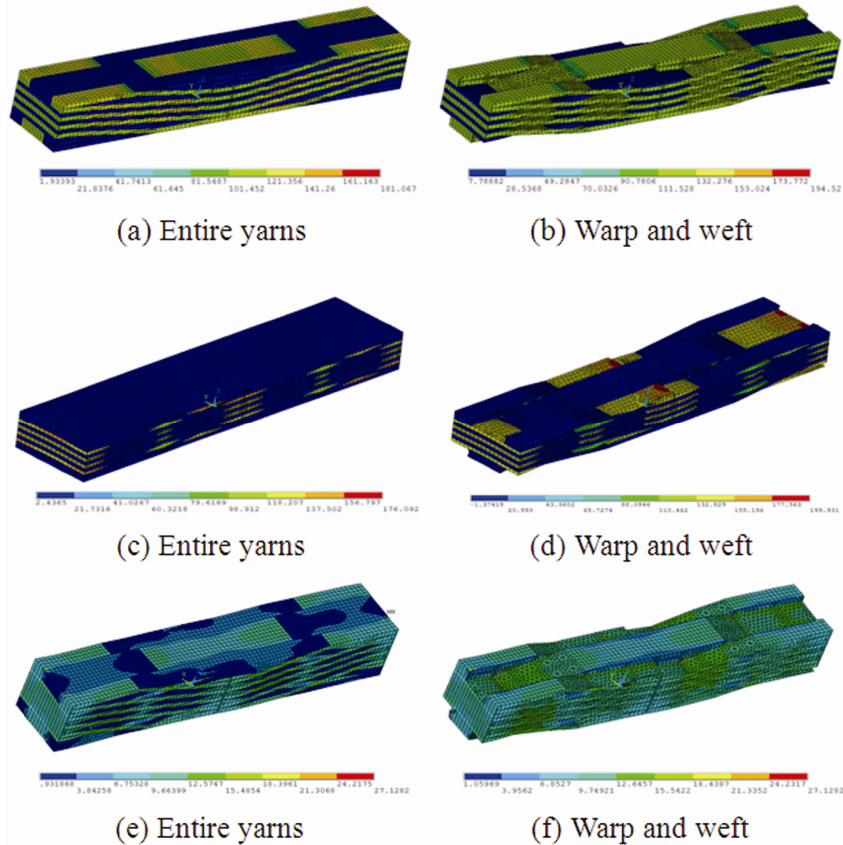


Fig. 7—Stress nephograms of FEM based on the full-cell model [(a) and (b) subjected to warp loading; (c) and (d) subjected to weft loading; and (e) and (f) subjected to in-plane shear loading]

It can be seen that under warp tensile loading, the stress levels in warp are obviously greater than that in weft and matrix, which reveals that the warps are the primary load-carrying objects subjected to the warp loading (Fig. 7). Meanwhile, an obvious stress concentration can be found in the inclined sections of warps closed to crossing points, which indicates the damages, such as micro-cracks, might be preliminarily generated in these regions [Fig. 7(b)].

According to Fig. 7(c), the wefts are the primary load-carrying objects under weft loading and the stress concentrations are focused on the outmost layer weft [Fig. 7(d)]. The possible reason is the squeezing effect of the outmost layer warp and secondary layer warp.

For the stress response of the full-cell model subjected to the in-plane shear loading, the stress distributions in warps and wefts are basically similar, but still greater than that in the matrix [Figs 7(e) and (f)]. Furthermore, due to the relatively longer warp, it leads to the extent of tensile and torsional deflection, which is more serious.

3.2 Discussion on Elastic Properties

Figure 8 illustrates the effect of thickness (L_z) and the fibre aggregation density (P_j) on the mechanical performance of fibre bundles, where the former can reflect the influence of processing technology and the later can be regarded as the fibre volume fraction in the unidirectional composites.

• Effect on Elastic Modulus E_x

In Fig. 8(a), it is clearly seen that the elastic modulus E_x increases basically by fixed amplitudes with the increase of P_j when L_z is certain. Additionally, according to Fig. 8(c), though both of the inclination angles in outmost layer and internal layer warps are increased linearly with the decrease of P_j , the E_x still experiences a decline trend. It suggests that the influence of the material parameter P_j on the modulus E_x is greater than that of the structural parameter L_z . However, when P_j is given, the modulus E_x decreases quasi-linearly as L_z increases, which indicates that the mechanical properties of 2.5D woven composites cannot be fully described by the Inner-cell model. Furthermore, the values calculated by FEM based

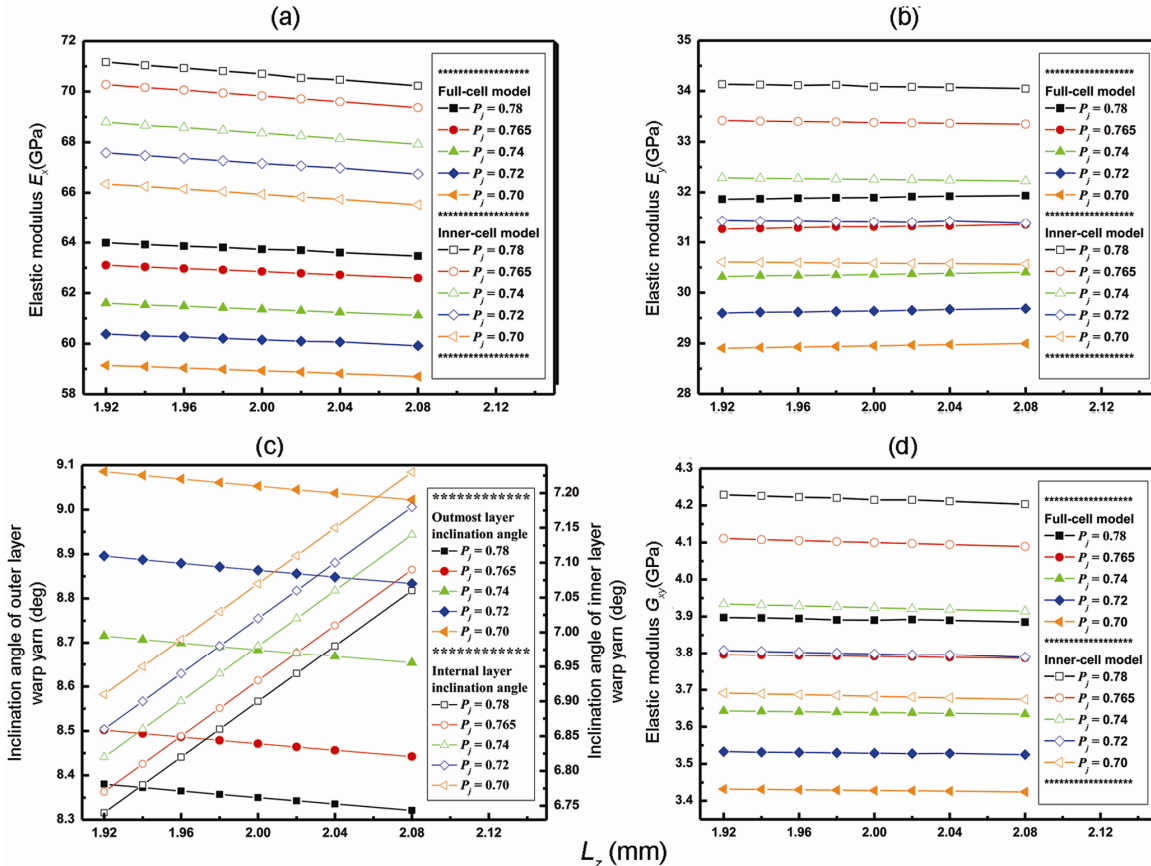


Fig. 8—Effect of fibre aggregation density in warp yarn and thickness on the elastic properties and inclination angle

Table 1—Material parameter of the specimens

Parameter	E_{f1}/E_m	E_{f2}	G_{f12}/G_m	G_{f23}	u_{f12}/u_m
T300-3K	230	40	17	4.8	0.3
QY8911-IV	4.16	—	—	—	0.34

Table 2—Woven parameter of the specimens

Specimen	M_w , tows/cm	M_s , tows/cm	N_f	N_h	L_z , mm	P_j
A	10	3.5	5	6	1.88	0.65
B	10	3.5	5	6	1.88	0.65

A and B represent the specimens subjected to warp and weft loading respectively.

Table 3—Predicted results in comparison with test data

Performance	No	Test results GPa	Average GPa	Discrete coefficient %	Prediction results			
					Full-cell model	Error %	Inner-cell model	Error %
E_x	1	58.78	60.77	3.08	61.01	0.39	66.36	9.20
	2	62.50						
	3	61.03						
E_y	4	33.84	33.73	2.61	30.04	11.20	30.28	10.49
	5	34.55						
	6	32.80						

on the Inner-cell model are greater than that based on the full-cell model.

- Effect on Elastic Modulus E_y

In Fig. 8(b), the elastic constant E_y is nearly horizontal lines as L_z increases when P_j is given, but the rise of P_j results in the increase of E_y obviously. The possible reason is that though there is an increase in thickness, the configuration and property are not affected. That is to say, the carry-loading areas of wefts are not increased remarkably.

- Effect on Elastic Modulus G_{xy}

The elastic property G_{xy} has a slight decrease with the increase of L_z [Fig. 8(d)]. The elastic modulus G_{xy} changes a little bit with the increase of L_z , which demonstrates that G_{xy} is thickness-independent for this type of material. In addition, the experimental results based on the Inner-cell model are greater than the related values based on the full-cell mode.

3.3 Comparison with Experimental Results

As stated above, a set of 6 specimens were prepared along the warp and weft directions to verify the analytical models. An MTS 810 hydraulic servo dynamic material test machine with a 25.4mm MTS-634-25 extensometer was used to perform the tests at room temperature (20°C). The material parameters and woven parameters of specimens are shown in Tables 1 and 2. The corresponding results are illustrated in Table 3.

Good coincidence between the experimental and theoretical results based on the full-cell model suggests the feasibility of the proposed model and

approach in predicting the elastic properties of 2.5D woven composites. Additionally, the prediction results based on the full-cell model are more close to the corresponding test results than those based on the Inner-cell model, especially the warp modulus. Therefore, it is more reasonable to consider the influence of the outmost layer structure on the mechanical properties.

4 Conclusion

In this work, a new predictive model called full-cell model for the elastic properties of 2.5D angle-interlock woven resin composites is proposed. The influence of fibre aggregation density and thickness on the mechanical properties of this material is then studied. Under the warp tensile loading, the modulus E_x is increased obviously with the increase of the packing factor P_j . However, it is decreased steady as L_z increases. For the cases of the weft and shear tensile, the values change in a similar tendency, which are increased monotonically as P_j increases, but tend to be constant when L_z is altered. Finally, there is a good agreement between the predicting results based on the full-cell model and the test results. More precise predicted results based on the full-cell model are obtained compared to those based on the Inner-cell model.

Acknowledgement

Authors are thankful for the funding support by Jiangsu Innovation Program for Graduate Education (grant number KYLX_0237)— the Fundamental Research Funds for the Central Universities.

References

- 1 Ayranci C & Carey J, *Compos Struct*, 85(1) (2008) 43.
- 2 Sankar B V & Marrey R V, *Compos Sci Technol*, 57(6) (1997) 703.
- 3 Zheng J, *Research on elastic property prediction and failure criteria of 2.5D woven composites*, PhD thesis, Nanjing University of Aeronautics and Astronautics, 2008.
- 4 Qiu R, *Research on fatigue life prediction and damage analysis of 2.5D woven composites*, PhD thesis, Nanjing University of Aeronautics and Astronautics, 2014.
- 5 Hallal A , Younes R , Fardoun F , F Fardoun & S Nehme, *Compos Struct*, 94(10) (2012) 3009.
- 6 Jiang Y, Tabiei A & Simites G J, *Compos Sci Technol*, 60(9) (2000) 1825.
- 7 Tan P , Tong L & Steven G P, *Compos Part A- Appl S*, 30(5) (1999) 637.
- 8 Ishikawa T & Chou T, *J Compos Mater*, 16(1) (1982) 2.
- 9 Ishikawa T & Chou T, *J Compos Mater, J Mater Sci*, 17(11) (1982) 3211.
- 10 Chou T & Ishikawa T, *AIAA J*, 21(12) (1983) 1714.
- 11 Z Lu, Y Zhou, Z Yang & Q Liu, *Comp Mater Sci*, 79 (2013) 485.
- 12 Zhou Y, Lu Z & Yang Z, *Compos Part B- Eng*, 47 (2013) 220.
- 13 Dong W F, Xiao J & Li Y, *Mat Sci Eng A- Struct*, 457 (2007) 199.
- 14 Xia Z H, Zhou C W, Yong Q L & Wang X, *Int J Solids Struct*, 43(2) (2006) 266.